Pergamon

Int. J. Heat Mass Transfer. Vol. 39, No. 12, pp. 2545–2557, 1996

0017–9310/96 $15.00 + 0.00

0017–9310(95)00246–4

Free convection fluid flow due to a periodically heated and cooled vertical flat plate embedded in a porous media

R. BRADEAN† and D. B. INGHAM
Department of Applied Mathematical Studies, The University of Leeds, Leeds, LS2 9JT, U.K.

P. J. HEGGS
Department of Chemical Engineering, UMIST, Manchester, M60 1QD, U.K.

and

I. POP
Faculty of Mathematics, The University of Cluj, R-3400 Cluj, CP 253, Romania

(*Received* 17 *December* 1994 *and in final form* 21 *June* 1995)

Abstract—In this paper we investigate the steady, two-dimensional, free convection flow caused by a sinusoidally heated and cooled infinite vertical surface that delimits a semi-infinite porous media. An analytical solution which is valid for small values of the Rayleigh number, Ra, is obtained using a regular perturbation method. A finite-difference technique is used to numerically solve the problem for $0 \leqslant Ra \leqslant 150$ and for small values of Ra, the results are in very good agreement with the analytical solutions and the streamlines are in the form of a row of counter rotating cells which are situated close to the vertical surface. As the Rayleigh number increases, above a value of about 40, then the cellular flow separates from the plate. At very large values of Ra, a scaling analysis has been performed and the results suggest that the vertical velocity and the local Nusselt number on the plate support better the boundary-layer scalings, than does the mean vertical velocity and the mean Nusselt number along the plate. In the situation in which the flow separates, i.e. for $Ra \gtrsim 40$, the smallest possible solution domain must be chosen, by using the symmetry of the problem, otherwise it has not been possible to obtain a convergent numerical solution. Copyright © 1996 Elsevier Science Ltd.

1. INTRODUCTION

Convective heat transfer in porous media is a topic of rapidly growing interest due to the wide range of geophysical and engineering applications, such as storage of radioactive nuclear waste materials, the exploration of petroleum and gas fields, the design of underground energy storage systems, insulation of buildings and equipment, engineering aspects of irrigation systems, etc. Many studies, with application to the above research areas, are gathered in a comprehensive review of convective heat transfer mechanisms through porous media in the book by Nield and Bejan [1].

Much attention has, in the past, been given to the free convection from a semi-infinite flat plate which is embedded in a porous media, whose temperature varies as some power of the distance from the leading edge of the plate. Similarity solutions have been extensively employed to solve the steady boundary-layer equations for such wall temperature distributions, see for example Cheng and Minkowycz [2] and Ingham and Brown [3]. Transient boundary-layer flows due to a heated or cooled vertical flat plate have also been investigated in many studies. Ingham *et al.* [4] considered the situation in which the impermeable surface, initially at constant temperature, is suddenly cooled to the same temperature as the ambient fluid. Similarly solutions for small and large values of time were matched by using a numerical technique and they found that there is an infinite number of possible solutions, each with algebraic decay. The case when there is an impulsive increase in the wall temperature was analysed by Cheng and Pop [5]. The governing equations for the growth of the boundary-layer thickness were obtained using the Karman–Pohlhausen integral method and the solution obtained exactly, using the method of characteristics and approximately using the method of integral relations.

The purpose of this paper is to investigate a relatively unknown class of steady, free convection flows, namely the flows caused by the heating and the cooling of an infinite flat plate which is embedded in a porous media. Poulikakos and Bejan [6] considered the con-

† On leave from Faculty of Mathematics, The University of Cluj, R-3400 Cluj, CP 253, Romania.

NOMENCLATURE

c	constant, equation (26)
d	non-dimensional distance from the plate
D	solution domain
g	acceleration due to gravity
G_Y	the grid system in the domain D_a
G_Z	the grid system in the domain D_c
K	permeability of the porous media
L	a characteristic length
$m+1$	number of nodal points in the x direction
$n+1$	number of nodal points in the y direction
Nu	Nusselt number, $= -(\partial T/\partial y)_{y=0}$
$p+1$	number of nodal points in the z direction
Ra	Rayleigh number, $= Kg\beta T_a L/\nu\alpha$
T	non-dimensional temperature, $=(\hat{T}-T_c)/T_a$
T_a	amplitude of the plate temperature oscillations
u, v	non-dimensional velocity components along x and y directions, $=\hat{u}/U_c$ and $\hat{v}/U_c$, respectively
U_c	a characteristic velocity, $= Kg\beta T_a/\nu$
x, y	non-dimensional Cartesian coordinates along and normal to the plate, $=\hat{x}/L$ and $\hat{y}/L$, respectively
z	transformed coordinate, equation (26).

Greek symbols

α	thermal diffusivity
β	coefficient of thermal expansion
ν	kinematic viscosity of the convective fluid
ψ	non-dimensional streamfunction
ε	convergence parameter
ω	relaxation factor.

Superscripts

$\hat{}$	dimensional variables
$\bar{}$	average quantities
$\tilde{}$	boundary-layer variables
s	order of iterations.

Subscripts

i, j	nodal points
m	the maximum absolute value along the plate
∞	condition at infinity.

figuration of a horizontal infinite flat plate having either a cosine or a step function form of temperature variation. In order to obtain a numerical solution the fixed temperature boundary condition at infinity was enforced at a very large distance from the plate, which depends on the value of the Rayleigh number, Ra. Numerical solutions were obtained using a finite-difference scheme and a scale analysis was performed to show that a row of counter rotating cells develops near the horizontal surface, which penetrates further into the porous media as the value of Ra increases. More recently, Bradean *et al.* [7] considered the same problem as Poulikakos and Bejan [6], when there is a cosine temperature variation along the horizontal plate, and showed that a fixed temperature boundary condition cannot be enforced at infinity since the temperature there is constant, but depends on the Rayleigh number. The appropriate boundary condition was found to be that of no heat transfer at an infinite distance from the plate. Analytical solutions for small values of the Rayleigh number and finite-difference results proved that this problem is one of infinite penetration and not finite as considered by Poulikakos and Bejan [6]. In a manner which is similar to the vertical situation, Poulikakos and Bejan [8] described the free convection flow in a porous media enclosed by a rectangular domain, due to a heated and cooled vertical side. The temperature distribution on the vertical differentially heated wall is assumed to be of the step function form, whereas the other three boundaries are insulated. A scale analysis and a finite-difference method were employed in two situations, namely when the side heating effect is positioned above and below the side cooling effect, and they showed, in each case, that the natural circulation consists of two counter rotating cells situated one above the other.

In this paper we analyse the free convection from an infinite vertical wall which is embedded in a porous media and having a sine temperature variation.

For small values of the Rayleigh number we present approximate analytical solutions for the governing equations using a series expansion method in terms of Ra and numerical solutions are obtained in the range $0 \leqslant Ra \leqslant 150$, using a finite-difference scheme. In this situation it is possible to have a constant temperature boundary condition at infinity and, in order to solve the problem numerically, this is enforced exactly at infinity using a scaling in the direction normal to the plate, as proposed by Zeldin and Schmidt [9]. The analytical and numerical results for the streamlines and isothem patterns, the mean fluid velocity along the plate and the mean Nusselt number are in very good agreement for small values of the Rayleigh number. The fluid separation from the plate and the development of a recirculation region as Ra increases above a value of about 40 is briefly analysed using

two variables, namely the vertical velocity and the horizontal temperature gradient along the plate. When Ra is very large, both the mean and the local flow characteristics are calculated from the numerical solution. The necessity of choosing the smallest solution domain possible due to the symmetry of the problem is discussed in order to obtain a convergent numerical solution.

2. GOVERNING EQUATIONS

In this paper we consider the two-dimensional steady, free convection fluid flow due to a heated and cooled vertical infinite flat plate which is embedded in a saturated porous media which is maintained at a constant temperature T_∞. We choose the $\hat{x}$ and $\hat{y}$ coordinates along and normal to the plate, respectively, and the temperature to have a sinusoidal distribution along the plate of the form

$$\hat{T} = T_a \sin(\hat{x}/L) + T_\infty, \tag{1}$$

where T_a and $2\pi L$ are the amplitude and the period of the wall temperature variations, respectively. If we assume that, (i) the convective fluid and the porous media are in local thermal equilibrium, (ii) the properties of the fluid and the porous media are constant, (iii) the Boussinesq approximation is valid and (iv) Darcy's law is applicable, the governing equations can be written in the form [3]

$$\frac{\partial^2\hat{\psi}}{\partial\hat{x}^2} + \frac{\partial^2\hat{\psi}}{\partial\hat{y}^2} = \frac{Kg\beta}{\nu}\frac{\partial\hat{T}}{\partial\hat{y}} \tag{2}$$

$$\frac{\partial^2\hat{T}}{\partial\hat{x}^2} + \frac{\partial^2\hat{T}}{\partial\hat{y}^2} = \frac{1}{\alpha}\left(\frac{\partial\hat{\psi}}{\partial\hat{y}}\frac{\partial\hat{T}}{\partial\hat{x}} - \frac{\partial\hat{\psi}}{\partial\hat{x}}\frac{\partial\hat{T}}{\partial\hat{y}}\right), \tag{3}$$

where $\hat{T}$ is the temperature, $\hat{\psi}$ is the streamfunction which is defined in the usual way, namely $\hat{u} = \partial\hat{\psi}/\partial\hat{y}$ and $\hat{v} = -\partial\hat{\psi}/\partial\hat{x}$, and $\hat{u}$ and $\hat{v}$ are the fluid velocities in the $\hat{x}$ and $\hat{y}$ directions, respectively; g is the acceleration due to gravity which is positive in the negative $\hat{x}$ direction; ν, β, K and α are the kinematic viscosity, the thermal expansion coefficient of the fluid, the permeability and the thermal diffusivity of the porous media, respectively.

We now define the dimensionless variables as follows

$$x = \hat{x}/L \quad y = \hat{y}/L \quad u = \hat{u}/U_c \quad v = \hat{v}/U_c \tag{4}$$

$$T = (\hat{T} - T_\infty)/T_a \quad \psi = \hat{\psi}/(U_c L), \tag{5}$$

where $U_c = Kg\beta T_a/\nu$ is a characteristic velocity. In terms of the new variables, equations (2) and (3) become

$$\frac{\partial^2\psi}{\partial x^2} + \frac{\partial^2\psi}{\partial y^2} = \frac{\partial T}{\partial y} \tag{6}$$

$$\frac{\partial^2 T}{\partial x^2} + \frac{\partial^2 T}{\partial y^2} = Ra\left(\frac{\partial\psi}{\partial y}\frac{\partial T}{\partial x} - \frac{\partial\psi}{\partial x}\frac{\partial T}{\partial y}\right), \tag{7}$$

where $Ra = Kg\beta T_a L/\nu\alpha$ is the Rayleigh number. Since the problem is periodic in the x direction we need only solve equations (6) and (7) in the domain

$$D = \{(x,y) \in E^2 : 0 \leqslant x \leqslant 2\pi \quad 0 \leqslant y < \infty\} \tag{8}$$

subject to the following boundary conditions

$$T(x,0) = \sin(x) \quad \psi(x,0) = 0 \quad 0 \leqslant x \leqslant \pi \tag{9a}$$

$$T(0,y) = T(2\pi,y) \quad \psi(0,y) = \psi(2\pi,y) \quad 0 \leqslant y < \infty \tag{9b}$$

$$T(x,y) \to 0 \quad \psi(x,y) \to 0 \quad \text{as } y \to \infty \quad 0 \leqslant x \leqslant \pi. \tag{9c}$$

Due to the reasons outlined in Section 5, it is more convenient to look for a solution for which $\psi = 0$ and $T = 0$ at $x = k\pi$, k integer. Then it can be easily proved that the temperature and the streamfunction are antisymmetric functions about the plane $x = \pi$, i.e. $T(x,y) = -T(2\pi - x,y)$ and $\psi(x,y) = -\psi(2\pi - x,y)$ where $0 \leqslant x \leqslant \pi$ and $0 \leqslant y < \infty$, and the problem reduces to solving equations (6) and (7) in the domain

$$D_0 = \{(x,y) \in E^2 : 0 \leqslant x \leqslant \pi \quad 0 \leqslant y < \infty\} \tag{10}$$

subject to the following boundary conditions:

$$T(x,0) = \sin(x) \quad \psi(x,0) = 0 \quad 0 \leqslant x \leqslant \pi \tag{11a}$$

$$T(x,y) = 0 \quad \psi(x,y) = 0 \quad x = 0,\pi \quad 0 \leqslant y < \infty \tag{11b}$$

$$T(x,y) \to 0 \quad \psi(x,y) \to 0 \quad \text{as } y \to \infty \quad 0 \leqslant x \leqslant \pi. \tag{11c}$$

3. ANALYTICAL SOLUTION

3.1. *Small Rayleigh number*

We look for a solution of equations (6) and (7), subject to the boundary conditions (9), which is valid for small values of Ra in the form

$$\psi = \psi_0 + Ra\psi_1 + (Ra^2)\psi_2 + 0(Ra^3) \tag{12a}$$

$$T = T_0 + RaT_1 + (Ra^2)T_2 + 0(Ra^3), \tag{12b}$$

where ψ_0, ψ_1, ψ_2 and T_0, T_1, T_2 are independent of the Rayleigh number. On substituting these expressions into the governing equations (6) and (7) and equating the same powers of the Rayleigh number we obtain the following partial differential equations:

$$\frac{\partial^2 T_0}{\partial x^2} + \frac{\partial^2 T_0}{\partial y^2} = 0 \tag{13a}$$

$$\frac{\partial^2\psi_0}{\partial x^2} + \frac{\partial^2\psi_0}{\partial y^2} = \frac{\partial T_0}{\partial y} \tag{13b}$$

$$\frac{\partial^2 T_1}{\partial x^2}+\frac{\partial^2 T_1}{\partial y^2}=\frac{\partial \psi_0}{\partial y}\frac{\partial T_0}{\partial x}-\frac{\partial \psi_0}{\partial x}\frac{\partial T_0}{\partial y} \tag{13c}$$

$$\frac{\partial^2 \psi_1}{\partial x^2}+\frac{\partial^2 \psi_1}{\partial y^2}=\frac{\partial T_1}{\partial y} \tag{13d}$$

$$\frac{\partial^2 T_2}{\partial x^2}+\frac{\partial^2 T_2}{\partial y^2}=\frac{\partial \psi_0}{\partial y}\frac{\partial T_1}{\partial x}-\frac{\partial \psi_0}{\partial x}\frac{\partial T_1}{\partial y}+\frac{\partial \psi_1}{\partial y}\frac{\partial T_0}{\partial x}-\frac{\partial \psi_1}{\partial x}\frac{\partial T_0}{\partial y} \tag{13e}$$

$$\frac{\partial^2 \psi_2}{\partial x^2}+\frac{\partial^2 \psi_2}{\partial y^2}=\frac{\partial T_2}{\partial y}. \tag{13f}$$

The problem reduces to solving, in turn, equations (13), subject to the boundary conditions

$$\psi_0(x,0)=0 \quad T_0(x,0)=\sin(x) \quad 0\leqslant x\leqslant \pi \tag{14a}$$

$$\psi_k(x,0)=0 \quad T_k(x,0)=0 \quad k=1,2,\ldots \quad 0\leqslant x\leqslant \pi \tag{14b}$$

$$\psi_k(0,y)=\psi_k(2\pi,y) \quad T_k(0,y)=T_k(2\pi,y) \quad k=0,1,\ldots \quad 0\leqslant y<\infty \tag{14c}$$

$$\psi_k(x,y)\to 0 \quad T_k(x,y)\to 0 \quad k=0,1,\ldots \quad y\to 0 \quad 0\leqslant x\leqslant \pi \tag{14d}$$

and we obtain

$$T_0=\mathrm{e}^{-y}\sin(x) \tag{15a}$$

$$\psi_0=\frac{1}{2}y\,\mathrm{e}^{-y}\sin(x) \tag{15b}$$

$$T_1=-\frac{1}{16}y\,\mathrm{e}^{-2y}\sin(2x) \tag{15c}$$

$$\psi_1=\frac{1}{64}\left(\frac{1}{2}y-y^2\right)\mathrm{e}^{-2y}\sin(2x) \tag{15d}$$

$$T_2=\left[\frac{3}{2048}\mathrm{e}^{-y}-\frac{1}{256}\left(\frac{3}{8}+y+y^2\right)\mathrm{e}^{-3y}\right]\sin(x)+\frac{1}{384}\left(\frac{1}{12}y+y^2\right)\mathrm{e}^{-3y}\sin(3x) \tag{15e}$$

$$\psi_2=\left[\frac{1}{4096}(-7+3y)\,\mathrm{e}^{-y}+\frac{1}{2048}\left(\frac{7}{2}+\frac{11}{2}y+3y^2\right)\mathrm{e}^{-3y}\right]\sin(x)-\frac{1}{768}\left(\frac{5}{72}y+\frac{1}{8}y^2-\frac{1}{3}y^3\right)\mathrm{e}^{-3y}\sin(3x). \tag{15f}$$

It is important to note that the boundary conditions (11) are satisfied, although the solution has been obtained using the boundary conditions (9). From this solution, analytical expressions for the mean velocity along the plate $\bar{u}$ and the mean Nusselt number $\overline{Nu}$ are obtained in the form

$$\bar{u}=\int_0^{\pi}u(x,0)\,\mathrm{d}x=1-\frac{5}{82944}Ra^2+0(Ra^3) \tag{16a}$$

$$\overline{Nu}=\int_0^{\pi}(-\partial T/\partial y)_{y=0}\,\mathrm{d}x=2+\frac{25}{13824}Ra^2+0(Ra^3). \tag{16b}$$

3.2. *Large Rayleigh number*

At large values of the Rayleigh number, Ra, a thermal boundary-layer is formed adjacent to the heated vertical plate. The boundary-layer equations are obtained by neglecting the second derivatives of ψ and T with respect to x in comparison to the second derivatives of ψ and T with respect to y in equations (6) and (7) [3], i.e.

$$\frac{\partial^2 \psi}{\partial y^2}=\frac{\partial T}{\partial y} \tag{17}$$

$$\frac{\partial^2 T}{\partial y^2}=Ra\left(\frac{\partial \psi}{\partial y}\frac{\partial T}{\partial x}-\frac{\partial \psi}{\partial x}\frac{\partial T}{\partial y}\right). \tag{18}$$

It is now convenient to introduce scaled variables as follows:

$$\psi=Ra^q\tilde{\psi} \quad T=Ra^t\tilde{T} \quad y=Ra^r\tilde{y} \tag{19}$$

where q, t and r are constants to be determined. Then equations (17) and (18) become

$$Ra^{q-2r}\frac{\partial^2 \tilde{\psi}}{\partial \tilde{y}^2}=\mathrm{Ra}^{t-r}\frac{\partial \tilde{\mathrm{T}}}{\partial \tilde{\mathrm{y}}} \tag{20}$$

$$Ra^{t-2r}\frac{\partial^2 \tilde{T}}{\partial \tilde{y}^2}=Ra^{1+q+t-r}\left(\frac{\partial \tilde{\psi}}{\partial \tilde{\mathrm{y}}}\frac{\partial \tilde{\mathrm{T}}}{\partial \mathrm{x}}-\frac{\partial \tilde{\psi}}{\partial x}\frac{\partial \tilde{T}}{\partial \tilde{y}}\right) \tag{21}$$

and the temperature boundary condition on the plate is

$$Ra^t\tilde{T}=\sin(x). \tag{22}$$

In order to maintain the balance between terms in the boundary-layer equations, the exponents of Ra in the terms of equations (20) and (21) must be equal and the boundary-layer scalings are found to be

$$\psi=Ra^{1/2}\tilde{\psi} \quad T=\tilde{T} \quad y=Ra^{1/2}\tilde{y}. \tag{23}$$

4. NUMERICAL SOLUTION

Since the solution domain extends to infinity in the y direction, we divide the domain D into two regions, namely,

$$D_a = \{(x,y) \in E^2 : 0 \leqslant x \leqslant 2\pi \quad 0 \leqslant y \leqslant d\} \tag{24}$$

$$D_b = \{(x,y) \in E^2 : 0 \leqslant x \leqslant 2\pi \quad D \leqslant y < \infty\}, \tag{25}$$

where d is a positive constant to be specified and $D = D_a \cup D_b$. Then the infinite domain D_b is transformed into a finite domain by using the scaling in the y direction proposed by Zeldin and Schmidt [9], namely,

$$z = 1 - \frac{1}{1+c(y-d)}, \tag{26}$$

where c is a parameter to be determined. Therefore, the domain D_b in the (x,y) plane is mapped into the domain

$$D_c = \{(x,z) \in E^2 : 0 \leqslant x \leqslant 2\pi \quad 0 \leqslant z \leqslant 1\} \tag{27}$$

in the (x,z) plane and the transformed equations (6) and (7) in the domain D_c are obtained in the form

$$\frac{\partial^2 \psi}{\partial x^2} + c^2(1-z)^4 \frac{\partial^2 \psi}{\partial z^2} + 2c^2(1-z)^3 \frac{\partial \psi}{\partial z} = c(1-z)^2 \frac{\partial T}{\partial z} \tag{28}$$

$$\frac{\partial^2 T}{\partial x^2} + c^2(1-z)^4 \frac{\partial^2 T}{\partial z^2} - 2c^2(1-z)^3 \frac{\partial T}{\partial z} = Rac(1-z)^2 \left(\frac{\partial \psi}{\partial z} \frac{\partial T}{\partial x} - \frac{\partial \psi}{\partial x} \frac{\partial T}{\partial z} \right). \tag{29}$$

Hence, the problem reduces to solving equations (6) and (7) in the domain D_a and equations (28) and (29) in the domain D_c subject to the following boundary conditions

$$T(x,y) = \sin(x) \quad \psi(x,y) = 0 \quad y = 0 \quad 0 \leqslant x \leqslant 2\pi \tag{30a}$$

$$T(0,y) = T(2\pi,y) \quad \psi(0,y) = \psi(2\pi,y) \quad 0 \leqslant y \leqslant d \tag{30b}$$

and

$$T(0,z) = T(2\pi,z) \quad \psi(0,z) = \psi(2\pi,z) \quad 0 \leqslant z \leqslant 1 \tag{30c}$$

$$T(x,z) = 0 \quad \psi(x,z) = 0 \quad z = 1 \quad 0 \leqslant x \leqslant 2\pi. \tag{30d}$$

Similarly, numerical solutions of the governing equations (6) and (7) are obtained in the domain D_0 subject to the boundary conditions (11). In this situation, equations (6) and (7) are solved in the domain

$$D_{0a} = \{(x,y) \in E^2 : 0 \leqslant x \leqslant \pi \quad 0 \leqslant y \leqslant d\} \tag{31}$$

and equations (28) and (29) in the domain

$$D_{0c} = \{(x,z) \in E^2 : 0 \leqslant x \leqslant \pi \quad 0 \leqslant z \leqslant 1\} \tag{32}$$

subject to the following boundary conditions

$$T(x,y) = \sin(x) \quad \psi(x,y) = 0 \quad y = 0 \quad 0 \leqslant x \leqslant 2 \tag{33a}$$

$$T(x,y) = 0 \quad \psi(x,y) = 0 \quad x = 0,\pi \quad 0 \leqslant y \leqslant d \tag{33b}$$

and

$$T(x,z) = 0 \quad \psi(x,z) = 0 \quad x = 0,\pi \quad 0 \leqslant z \leqslant 1 \tag{33c}$$

$$T(x,z) = 0 \quad \psi(x,z) = 0 \quad z = 1 \quad 0 \leqslant x \leqslant 2. \tag{33d}$$

The numerical solution of the equations (6), (7), (28) and (29), subject to the boundary conditions (30), is obtained by using a finite-difference method. The discretization in the domain D_a consists of a rectangular grid G_y containing $m+1$ points $\{x_1 = 0, x_2, \ldots, x_m, x_{m+1} = \pi\}$ in the x direction and $n+1$ points $\{y_1 = 0, y_2, \ldots, y_n, y_{n+1} = d\}$ in the y direction. In the domain D_c we take a grid G_z of $m+1$ points $\{x_1 = 0, x_2, \ldots, x_m, x_{m+1} = \pi\}$ in the x direction and $p+1$ points $\{z_{n+1} = 0, z_{n+2}, \ldots, z_{n+p}, z_{n+p+1} = 1\}$ in the z direction. Consider now two points of the grid G_z located in the domain D_c at $(x_i, 0)$ and (x_i, z_{n+2}), $i \in \{1,2,\ldots,m+1\}$. These points are transformed in the domain D_b into (x_i, d) and (x_i, y_{n+2}). The link between grids G_y and G_z is made by choosing the parameter c such that

$$y_{n+2} - d = \frac{d}{n}, \tag{34}$$

where d/n is the step size in the y direction in grid G_y and using transformation (26) we obtain

$$c = \frac{n}{d(p-1)} \tag{35}$$

The finite-difference approximation of the partial differential equations (6), (7), (28) and (29) has been implemented by using the central-difference method. The discretization of the governing equations and the boundary conditions leads to a system of non-linear algebraic equations, which are solved using the successive over relaxation iterative method. The maximum difference between two successive iterations of the streamfunction and temperature is defined by

$$\Delta\psi^{(s)} = \max\{|\psi_{i,j}^{(s)} - \psi_{i,j}^{(s-1)}| : i = 1,2,\ldots,m+1 \quad j = 1,2,\ldots,n+p+1\} \tag{36a}$$

$$\Delta T^{(s)} = \max\{|T_{i,j}^{(s)} - T_{i,j}^{(s-1)}| : i = 1,2,\ldots,m+1 \quad j = 1,2,\ldots,n+p+1\}, \tag{36b}$$

where the notation $(\,)_{i,j}$ means the value of the function at the grid point (x_i, y_j) or (x_i, z_j) and the subscript s

denotes the order of the iteration. The iterative procedure is terminated when $\Delta\psi^{(s)}$ and $\Delta T^{(s)}$ are both smaller than some prescribed small value ε, say $\varepsilon = 10^{-8}$.

Third-order approximate formulae for the vertical fluid velocity $u = \partial\psi/\partial y$ and the horizontal temperature gradient $\partial T/\partial y$ at the mesh points on the boundary $y = 0$, are obtained using Taylor's expansion and equations (6) and (7) evaluated at $y = 0$. Then the mean velocity along the plate and the mean Nusselt number are calculated from the numerical solution for the streamfunction and the temperature using Simpson's formula.

5. RESULTS AND DISCUSSION

Numerical results of equations (6) and (7) in the domain D subject to the boundary conditions (9) have been obtained using the central-difference method in the range of values of the Rayleigh number $0 \leqslant Ra \leqslant 30$. The rate of convergence of the iterative method was found to be reasonably rapid and a relaxation factor of $\omega = 1.95$ can be used for $Ra = 0.25$, whereas a value of $\omega = 1.8$ is required for $Ra = 30$. In all the cases considered, the maximum difference between two successive iterations in the values of ψ and T, namely $\Delta\psi$ and ΔT, respectively, becomes less than $\varepsilon = 10^{-8}$ in less than 5000 iterations. In order to check the independency of the numerical solution on the mesh size, the mean velocity along the plate and the mean Nusselt number were calculated for two different grid systems, namely when there are 80–80–30 and 160–160–60 mesh points in the x, y and z directions, respectively. It was found that the values of $\bar{u}$ and $\overline{Nu}$ calculated using these grid systems agree within 0.01% for $Ra = 0.25$ and 1% for $Ra = 25$. Numerical solutions were calculated for different values of d and we found that for $d \geqslant 2\pi$ the numerical solution obtained is almost independent of d. Consequently, all the numerical results presented in this paper are for the 160–160–60 grid system with $d = 2\pi$.

For very small values of the Rayleigh number the analytical solution, which was obtained in Section 3, is used to check the accuracy of the numerical solution. Table 1, which presents the values of the mean velocity along the plate and the mean Nusselt number calculated analytically and numerically for $Ra = 0.25$, 1, 5 and 10, shows that for very small values of Ra, e.g. $Ra = 0.25$, there is very good agreement, within 0.02%, between the analytical and numerical solutions. As the Rayleigh number increases, the analytical solution, which is accurate to $0(Ra^3)$, becomes less accurate and, therefore, the analytical and numerical results become less consistent. However, they agree within 1% up to $Ra = 10$ and this is because the coefficients of the powers of Ra in the analytical solution decrease rapidly as the power of Ra increases.

Numerical solutions in the domain D have been obtained using the boundary conditions (9), but since the solutions also satisfy the boundary conditions (11), i.e. $\psi \approx 0$ and $T \approx 0$ at $x = 0$, π and 2π, and $\psi(x, y) \approx -\psi(2\pi - x, y)$ and $T(x, y) \approx -T(2\pi - x, y)$ for any $(x, y) \in D_0$, the results are only presented in the domain D_0. Figure 1 shows the evolution of the streamline and isotherm patterns for $Ra = 0.25$ and 25 as obtained from the numerical solution. It is seen in Fig. 1a that for small values of the Rayleigh number the hot temperature along the plate ($0 \leqslant x \leqslant \pi$) generates an upward stream of fluid which meets the downward flowing stream formed along the cold part of the plate ($\pi \leqslant x \leqslant 2\pi$). This results in a horizontal stream being formed along the plane $x = \pi$ which must turn around to fill the vacuum created near the points $x = 0$ and $x = 2\pi$ on the plate. Therefore a row of counter rotating cells develop along the plate. As the Rayleigh number increases, each cell makes contact with the vertical plate via the slender boundary-layer regions. The ability of the two adjacent cells to transfer heat into and out of the porous media and between them increases with increasing values of the Rayleigh number, see Fig. 1c, d. The vertical fluid velocity $u = (\partial\psi/\partial y)_{y=0}$ and the horizontal temperature gradient $(\partial T/\partial y)_{y=0}$ on the plate are plotted as a function of the distance along the plate in Fig. 2a, b, respectively, for $Ra = 0.25$, 10 and 25. As the Rayleigh number increases, the velocity near the location $x = \pi$ on the plate decreases while the maximum velocity on the plate increases. Therefore, near the location $x = \pi$ on the plate, a region where the velocity is very small is formed as the Rayleigh number increases, despite the fact that stronger streams are coming towards this point on the plate. This result is not surprising, since the only force acting in the present problem, namely, the buoyancy force, is proportional to the horizontal temperature gradient. In the neighbourhood of the location $x = \pi$ on the plate in the domain D_0, the horizontal temperature gradient which is negative for $Ra = 0.25$ becomes positive for $Ra = 25$, see Fig. 2b. Therefore, as the value of Ra increases, the upward flowing stream, formed along the hot part of the plate, is deflected near the location $x = \pi$ on the plate by the buoyancy force which acts downwards.

Table 1. The mean velocity and the mean Nusselt number calculated analytically (A) and numerically (N) as a function of the Rayleigh number

Ra		$\bar{u}$	$\overline{Nu}$
0.25	A	1.0000	2.0001
	N	1.0000	1.9999
1	A	0.9999	2.0018
	N	1.0000	2.0016
5	A	0.9985	2.0452
	N	0.9986	2.0444
10	A	0.9940	2.1808
	N	0.9951	2.1678

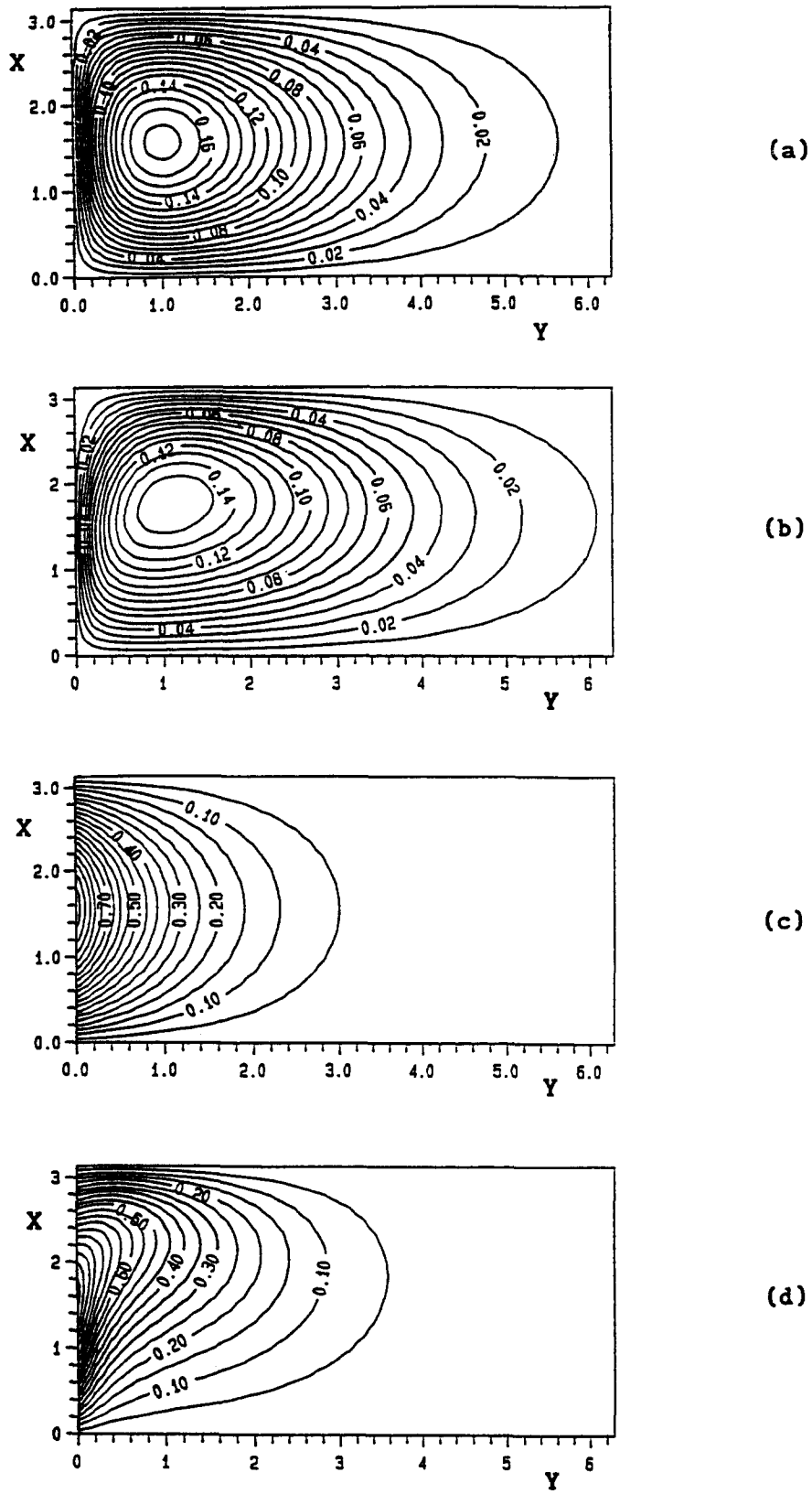

Fig. 1. Streamlines (a), (b), and isotherms (c), (d), in the domain D_{0a} for $Ra = 0.25$ and 25, respectively.

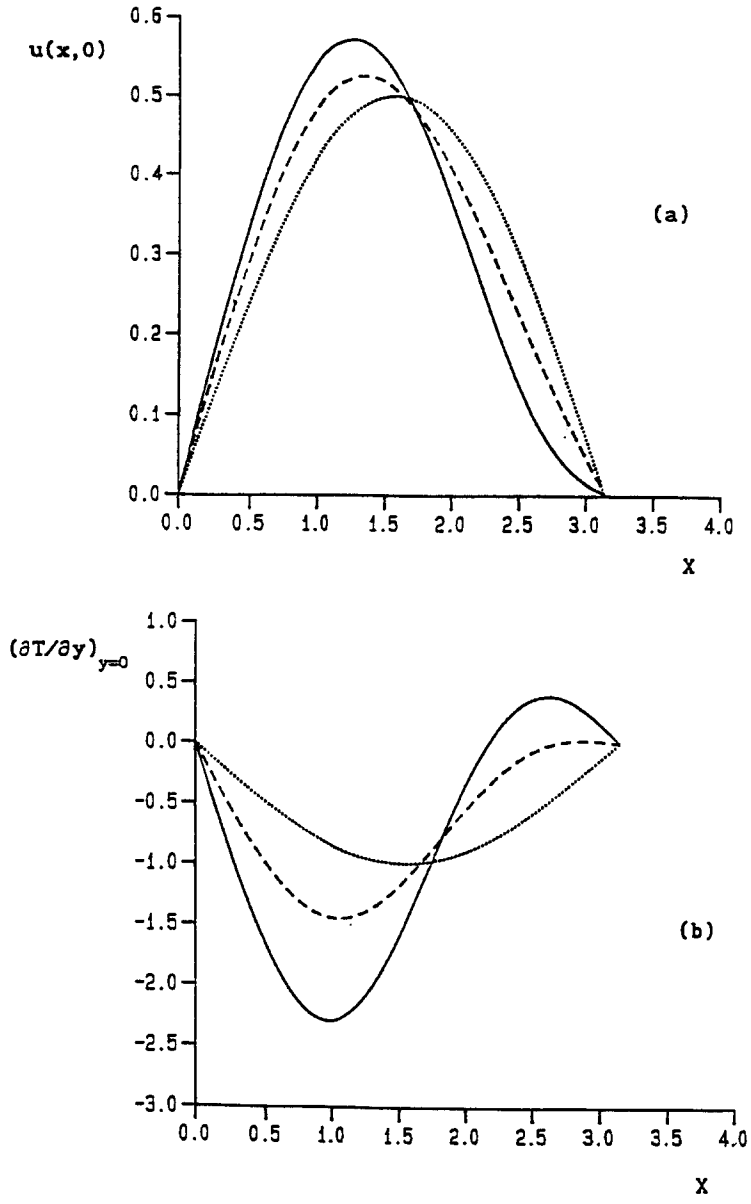

Fig. 2. The vertical velocity (a) and the horizontal temperature gradient (b) as a function of the distance along the plate. ..... $Ra = 0.25$, – – – $Ra = 10$ and —— $Ra = 25$.

We now consider situations of Rayleigh number in the range $30 < Ra \leqslant 150$. However, when $Ra \gtrsim 40$ the iterative procedure does not converge with the maximum difference between two successive iterations of ψ and T, namely $\Delta\psi$ and ΔT, respectively, being never less than $0(10^{-3})$ but oscillatory in nature. Numerical calculations were also performed using the first-order upwinding method, but we found the same oscillatory behaviour in the iterative procedure. We know from experience that, when dealing with strong convection problems, many methods give artificial oscillations in some regions of the solution domain, see for example Leonard [10]. However, these oscillations usually occur in central-difference and second- and third-order upwinding (QUICK) schemes rather than in first-order schemes. Leonard [10] eliminated artificial oscillations from the problem by developing the QUICK method, which is a third-order accurate scheme based on a quadratic upstream interpolation. The resulting method was found by using an exponential upstream interpolation, instead of quadratic, and is known as the SHARP scheme. Both the QUICK and the SHARP methods have been employed on this problem but we were still unable to obtain convergent results.

We found that the only way to numerically solve the problem for $Ra \gtrsim 40$ is to look for solutions for which $\psi = 0$ and $T = 0$ on $x = k\pi$, k integer, conditions which were satisfied for $Ra \lesssim 40$, and reduce the solution domain from D to D_0. Therefore, numeri-

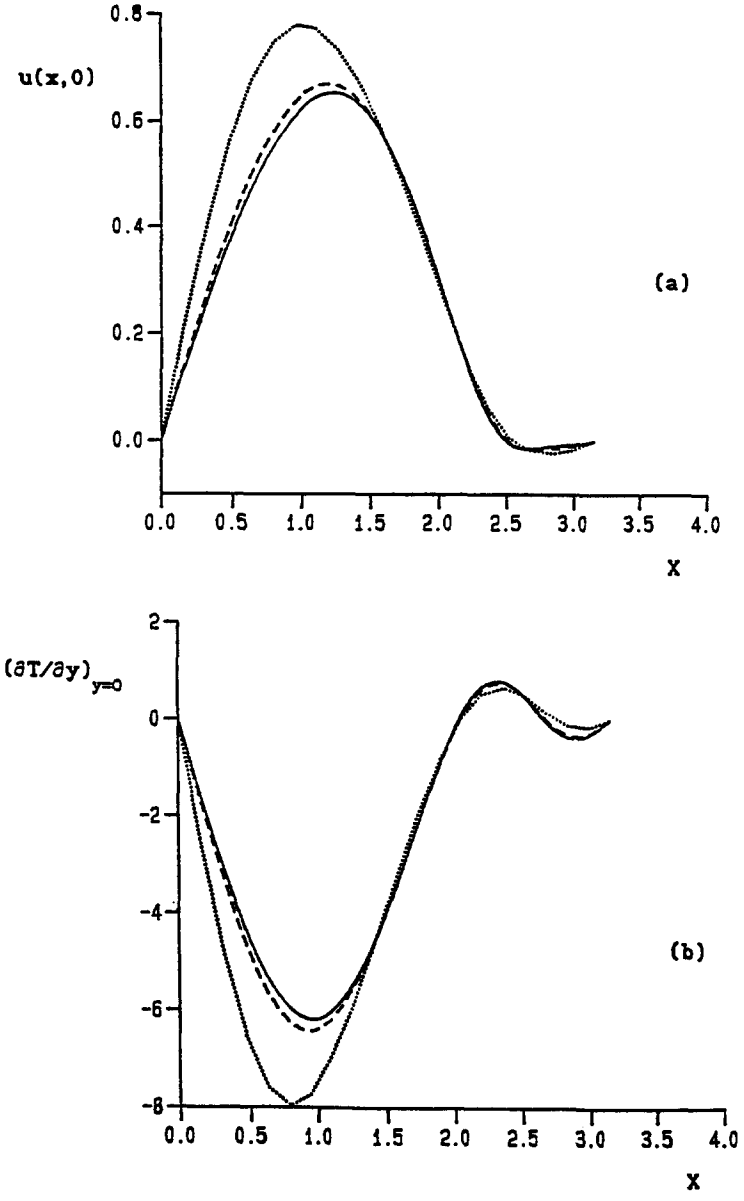

Fig. 3. The vertical velocity (a) and the horizontal temperature gradient (b) as a function of the distance along the plate for $Ra = 150$ obtained using the three grid systems; ..... 20–40–15, – – – 40–80–30 and —— 80–160–60 points being used in the x, y and z directions, respectively.

cal solutions for $30 < Ra \leqslant 150$ are obtained solving equations (6) and (7) in the domain D_0, subject to the boundary conditions (11). However, the accuracy of the numerical method is affected as the Rayleigh number increases, and the values of $\bar{u}$ and $\overline{Nu}$ calculated using the 40–80–30 and 80–160–60 grid systems which agree within 1% for $Ra = 25$, agree only within 4% for $Ra = 150$. The vertical velocity and the horizontal temperature gradient on the plate are plotted as a function of the distance along the plate in Fig. 3a, b, respectively, for $Ra = 150$ using three grid systems of 20–40–15, 40–80–30 and 80–160–60 point in the x, y and z directions, respectively. The value of $Ra = 150$ is the largest Rayleigh number investigated in this paper and, therefore, the results presented in Fig. 3 illustrate the largest errors involved. It can be seen that, as the mesh size decreases, the solutions appear to be tending to a limit, and all the numerical results presented in this paper are for the grid system of 80–160–60 points in the x, y and z directions, respectively.

The streamlines and isotherms are presented in Figs 4 and 5, respectively, for $Ra = 50$, 100 and 150 and the vertical velocity and the horizontal temperature gradient on the plate are plotted as a function of the distance along the plate in Fig. 6a, b, respectively, for $Ra = 25$, 50, 75, 100, 125 and 150. We observe that a recirculation develops near $x = \pi$ on the plate, as the Rayleigh number increases above a value of about 40.

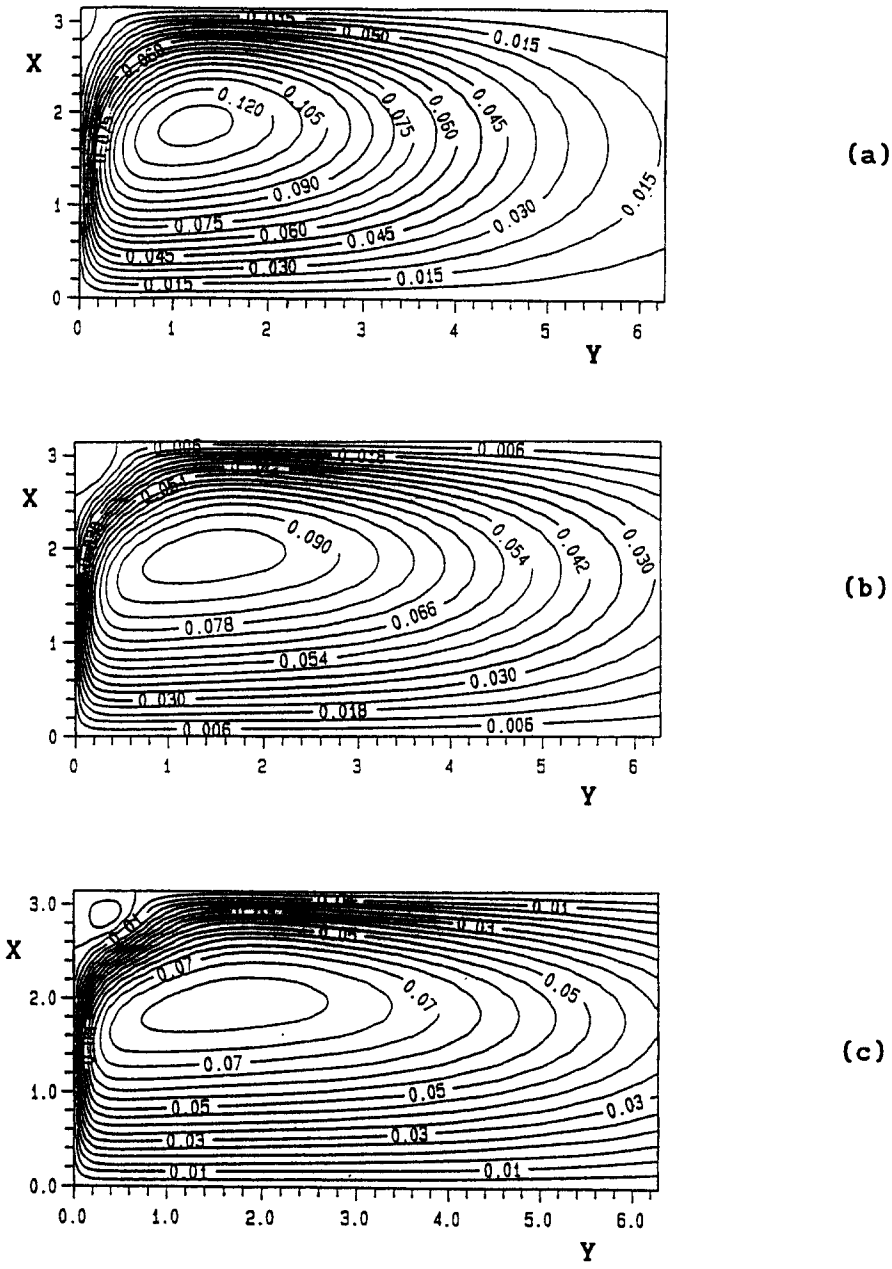

Fig. 4. Streamlines in the domain D_{0a} for $Ra = 50$, 100 and 150.

This is because the temperature gradient on the plate is positive in the neighbourhood of the location $x = \pi$, and negative elsewhere. Actually, the temperature gradient on the plate becomes positive in the neighbourhood of the point $x = \pi$ above a value of about $Ra = 10$, see Fig. 2b. Since the buoyancy force is proportional to the temperature gradient, then near the point $x = \pi$ on the plate this force acts downwards whilst elsewhere near the plate acts upwards. The buoyancy force acting upwards is stronger than the force acting downwards. For $10 \lesssim Ra \lesssim 40$, the effect of the buoyancy force in the neighbourhood of $x = \pi$ on the plate is to slow down the stream coming upwards near the point $x = \pi$. However, for $40 \lesssim Ra \lesssim 150$ the buoyancy force becomes sufficiently strong so as to pull the fluid downwards near the location $x = \pi$ on the plate and to make the main stream flowing upwards along the plate separate before it reaches the location $x = \pi$. This results in a bicellular flow in the domain D_0, i.e. a main cell rotating clockwise and a smaller cell which is situated near the point $x = \pi$ on the plate which is rotating counterclockwise. For $100 \lesssim Ra \lesssim 150$ the horizontal temperature gradient on the plate becomes negative again very close to the location $x = \pi$ and its absolute value increases with increasing Ra, see Fig. 6b. The

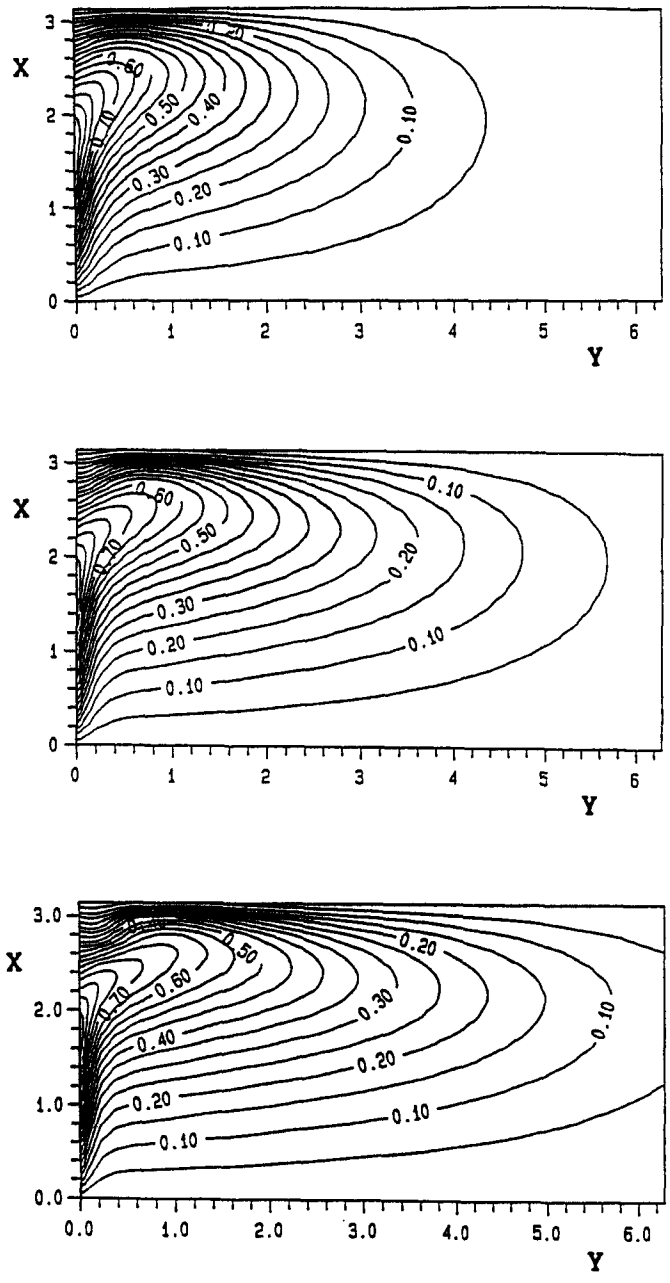

Fig. 5. Isotherms in the domain D_{0a} for $Ra = 50$, 100 and 150.

buoyancy force now acts upwards on the fluid situated very close to the location $x = \pi$ on the plate and this makes the recirculation already developed to rotate in a larger region from the plate as the Rayleigh number increases, see Fig. 4, while the velocity on the plate decreases in the neighbourhood of the location $x = \pi$, see Fig. 6a. When the Rayleigh number was increased above a value of about $Ra = 150$ we were unable to obtain a convergent numerical solution. Therefore, above a value of about $Ra = 150$ it is postulated that the recirculation region detaches from the vicinity of the plate and the steady state model is no longer appropriate, i.e. the unsteady problem should be considered.

At large values of the Rayleigh number, the boundary-layer scalings suggest that the velocity and the horizontal temperature gradient along the plate should be scaled as

$$\frac{\partial \tilde{T}}{\partial \tilde{y}} = \frac{\partial T}{\partial y} Ra^{-1/2} \quad y = 0 \quad 0 \leqslant x \leqslant \pi \tag{37a}$$

$$\frac{\partial \tilde{\psi}}{\partial \tilde{y}} = \frac{\partial \psi}{\partial y} \quad y = 0 \quad 0 \leqslant x \leqslant \pi, \tag{37b}$$

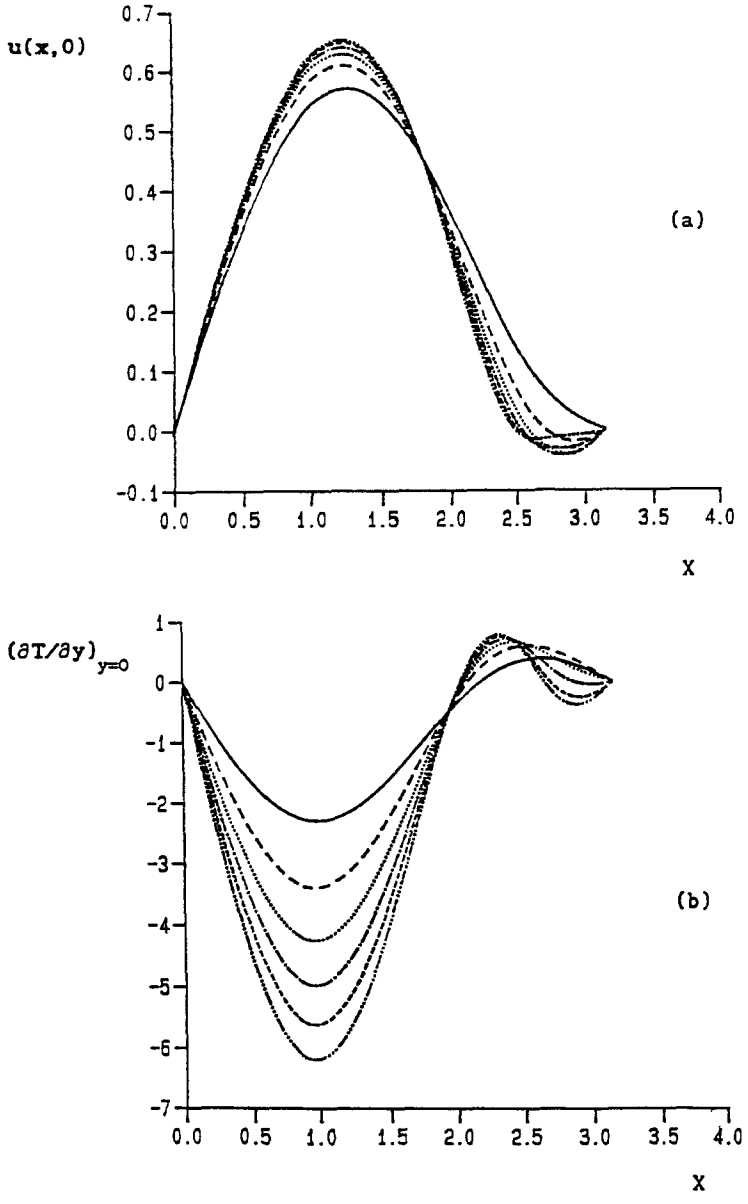

Fig. 6. The vertical velocity (a) and the horizontal temperature gradient (b) as a function of the distance along the plate for —— $Ra = 25$, – – – $Ra = 50$, ... $Ra = 75$, – · – · – · $Ra = 100$, - - - - $Ra = 125$, – · · – · · – · · $Ra = 150$.

where $\sim$ denotes the boundary-layer approximation. The values of $\bar{u} = \tilde{u}$, $\overline{Nu}$ and $\tilde{N}u = \overline{Nu}/Ra^{1/2}$ as calculated from the numerical solution are presented in Table 2 for $Ra = 50$, 75, 100, 125 and 150. These results show that as the Rayleigh number increases, the heat transfer processes intensifies near the plate,

Table 2. Some mean boundary-layer flow characteristics as a function of the Rayleigh number

Ra	$\bar{u} = \tilde{u}$	$\overline{Nu}$	$\tilde{N}u$
50	0.9676	3.0939	0.5521
75	0.9618	4.9452	0.5710
100	0.9613	5.9059	0.5906
125	0.9652	6.7822	0.6066
150	0.9718	7.5305	0.6149

Table 3. Some local boundary-layer flow characteristics as a function of the Rayleigh number

Ra	$u_m = \tilde{u}_m$	Nu_m	$\tilde{N}u_m$
50	0.6102	3.3960	0.4803
75	0.6296	4.2569	0.4915
100	0.6412	4.9842	0.4984
125	0.6487	5.6238	0.5030
150	0.6537	6.2001	0.5062

whereas the mean velocity along the plate almost approaches a constant value. The values of $\tilde{u}$ and $\tilde{Nu}$ from Table 2 also indicate that the scaling laws are satisfied by the numerical calculations.

Since the boundary-layer formed adjacent to the vertical plates separates from the plate between $x = \pi/2$ and $x = \pi$, the boundary-layer approximations are no longer valid in the neighbourhood of the location $x = \pi$ on the plate. Therefore, it is expected that the maximum value of the vertical velocity, u_m, and the local Nusselt number $[Nu = -(\partial T/\partial y)_{y=0}]$, Nu_m, along the plate support better the boundary-layer scalings and this is illustrated in Table 3 which contains the values of $\tilde{u}_m = u_m$, Nu_m and $\tilde{Nu}_m = Nu_m/Ra^{1/2}$ for $Ra = 50$, 75, 100, 125 and 150. It is also observed that when $Ra \gtrsim 50$ the locations where the vertical velocity and the horizontal temperature gradient along the plate have their maximum value does not depend on the value of the Rayleigh number.

6. CONCLUSIONS

In this study we have analysed the steady, free convection fluid flow through a semi-infinite porous media due to a heated and cooled vertical surface. For small values of Ra we showed analytically and numerically that near the periodically heated and cooled wall, the flow consists of a row of counter rotating cells which penetrates further into the porous media as the Rayleigh number increases. When the Rayleigh number is sufficiently large ($Ra \gtrsim 40$), the flow separates and two recirculating flow regions develop near a region of the wall where two streams formed along successive hot and cold regions of the wall meet. As the Rayleigh number increases, each main cell (i.e. not a recirculating cell) makes contact with the vertical plate via slender boundary-layer regions, and the ability of two adjacent cells to transfer heat into and out of the porous media and between them increases. The recirculating regions near the plate show a tendency to detach from the plate as Ra increases above a value of about 100. When the Rayleigh number is very large, the boundary-layer scalings for the vertical velocity and the local Nusselt number on the plate calculated in the region where the boundary-layer approximations are valid, are confirmed by the numerical solution. However, for $Ra \gtrsim 40$, the flow is probably unstable in the region where the separation occurs due to the development of two adjacent, counter rotating recirculations, and when the governing equations are solved in a domain which includes these two adjacent recirculating regions we are unable to obtain a convergent numerical solution.

REFERENCES

1. D. A. Nield and A. Bejan, *Convection in Porous Media*. Springer, New York (1992).
2. P. Cheng and W. J. Minkowycz, Free convection about a vertical flat plate embedded in a porous medium with application to heat transfer from a dike, *J. Geophys. Res.* **82,** 2040–2044 (1977).
3. D. B. Ingham and S. N. Brown, Flow past a suddenly heated vertical plate in a porous medium, *Proc. R. Soc. Lond.* **A403,** 51–80 (1986).
4. D. B. Ingham, J. H. Merkin and I. Pop, Flow past a suddenly cooled vertical flat surface in a saturated porous medium, *Int. J. Heat Mass Transfer* **25,** 1916–1919 (1982).
5. P. Cheng and I. Pop, Transient free convection about a vertical flat plate embedded in a porous medium, *Int. J. Engng Sci.* **22,** 253–264 (1984).
6. D. Poulikakos and A. Bejan, Penetrative convection in porous medium bounded by a horizontal wall with hot and cold spots, *Int. J. Heat Mass Transfer* **27,** 1749–1757 (1984).
7. R. Bradean, D. B. Ingham, P. J. Heggs and I. Pop, Buoyancy-induced flow adjacent to a periodically heated and cooled horizontal surface in porous media, *Int. J. Heat Mass Transfer* **39,** 615–630 (1996).
8. D. Poulikakos and A. Bejan, Natural convection in a porous layer heated and cooled along one vertical side, *Int. J. Heat Mass Transfer* **27,** 1879–1891 (1984).
9. B. Zeldin and F. W. Schmidt, Developing flow with combined forced-free convection in an isothermal vertical tube, *J. Heat Transfer* **94,** 211–223 (1972).
10. B. P. Leonard, Simple high-accuracy resolution program for convective modelling of discontinuities, *Int. J. Numer. Methods Fluids* **8,** 1291–1318 (1988).